piR-651 promotes tumor formation in non-small cell lung carcinoma through the upregulation of cyclin D1 and CDK4

DAN LI, YINGQUAN LUO, YAWEN GAO, YUE YANG, YINA WANG, YAN XU, SHENGYU TAN, YUWEI ZHANG, JUAN DUAN and YU YANG

Department of Geriatrics, The Second Xiangya Hospital of Central South University, Changsha, Hunan 410011, P.R. China

Received May 22, 2015; Accepted June 10, 2016

DOI: 10.3892/ijmm.2016.2671

Abstract. Piwi-interacting RNAs (piRNAs or piRs) are a novel class of non-coding RNAs that participate in germline development by silencing transposable elements and regulating gene expression. To date, the association between piRNAs and non-small cell lung carcinoma (NSCLC) has not yet been elucidated. In the present study, we have demonstrated that a significant increase in piR-651 expression occurs in NSCLC. Furthermore, the abnormal expression of piR-651 was associated with cancer progression in the patients with NSCLC. The upregulation of piR-651 in A549 cells caused a significant increase in cell viability and metastasis. The percentage of arrested cells in the G0/G1 phase was lower after piR-651 overexpression compared with the controls. We also examined the expression of oncogenes and cancer suppressor genes following piR-651 overexpression in NSCLC cells. Only the expression levels of cyclin D1 and CDK4 significantly correlated with piR-651 expression both *in vivo* and *in vitro*. Furthermore, by injecting nude mice with A549 cells transfected with piR-651 plasmids to establish a xenograft model, we demonstrated that there was a correlation between piR-651 overexpression and tumor growth, which was mediated by cyclin D1 and CDK4. These findings strongly support the notion that piR-651 induces NSCLC progression through the cyclin D1 and CDK4 pathway and it may have applications as a potential diagnostic indicator and therapeutic target in the management of NSCLC.

Introduction

Lung cancer is the leading cause of cancer-related deaths worldwide, and studies on lung cancer have increased significantly in recent years. Among all types of lung cancer, non-small cell lung carcinoma (NSCLC) represents the highest number of cases of diagnosed lung cancer (1). Surgical resection, chemotherapy and radiotherapy are currently used for the treatment of NSCLC (2). However, the long-term survival for NSCLC patients remains poor. A lack of information regarding the effects of genetic, epigenetic and environmental factors in NSCLC has led to difficulties in elucidating the developmental mechanisms of cancer cells, such as roles in viability, aggressiveness and progression. To date, improvements in the understanding of the genetic processes involved in NSCLC has assisted in the diagnosis and the establishment of treatment options. Unveiling the pathogenesis of lung cancer epigenetically would also aid in identifying new diagnostic biomarkers as well as in establishing new therapeutic strategies.

In cancer, the cellular genomes are unstable and typically exhibit alterations including amplification and/or deletion of cancer genes and epigenetic silencing (3). Epigenetic alterations including microRNA (miRNA or miR) silencing, DNA methylation and histone modification have been demonstrated to participate in cancer progression (4). DNA hypomethylation largely affects intergenic and intronic regions of the genome as well as repeat sequences and transposable elements (TEs) (5). In addition, the methylation levels of oncogenes and tumor suppressor genes in cancer cells are commonly aberrant (6). TEs as mobile factors in the genome are widely distributed among all regions, causing deleterious mutations, gene disruptions and chromosomal rearrangements (7), and potentially lead to the initiation and progression of cancer (8). To date, our understanding of the association between TEs and human cancer is limited. In addition, the correlation between the mobility of TEs and the cancer cell environment remains-unknown.

Recently, the piwi-interacting RNA (piRNA or piR) pathway was identified in germline cells in the testis and confirmed as an highly conserved, evolutionarily pathway in animals (9). piRNAs are 26-32 nucleotides in length and bind PIWI proteins and mediate the post-translational activities of TEs as well as gene expression (10-12). Thus, the piRNA pathway plays a crucial role in epigenetic change by regulating genome stability. Several PIWI-like genes have been identified as mammalian paralogs, including four paralogs in humans and three paralogs in the mouse (13). The initial studies of PIWI and piRNAs were focused on germ cell development, particularly in the testis. A recent study by Yan *et al* using high-throughput small RNA sequencing, showed widespread expression of piRNAs in

Correspondence to: Dr Yu Yang, Department of Geriatrics, The Second Xiangya Hospital of Central South University, 86 Renmin Road, Changsha, Hunan 410011, P.R. China
E-mail: yuyang_yy15@163.com

Key words: Piwi-interacting RNA, non-small-cell lung carcinoma, piR-651, tumor formation, cyclin D1, CDK4

somatic tissues, which suggested new functions of the piRNAs in addition to their roles in the development of gonads (14). These results suggest that the piRNA pathway has comprehensive functions during development, both in germ cells and somatic cells, by regulating TEs and gene expression.

Several studies have indicated that the piRNA pathway is increased in different types of cancer, including lung cancer, pancreatic cancer and ovarian cancer (15). The abundant expression of PIWI proteins has been found in the breast, gastrointestinal tract, stomach, and endometrium with cancer whereas no expression has been found in normal tissues (16,17). Moreover, increasing Piwil1 enhanced tumor growth and mortality (18). Piwil2 is also widely expressed in pre-cancerous stem cells, breast cancer cells and cervical cancer cells, suggesting that Piwil2 is involved in tumorigenesis (19). Piwil3 and Piwil4 expression has only been identified in colon cancer, to the best of our knowledge (16). In addition to PIWI proteins, piRNAs have also been found to be abnormally expressed in cancer cells. Cheng *et al* showed that piR-651 was upregulated in gastric cancer tissues and was associated with the tumor-node-metastasis (TNM) stage. The authors concluded that piR-651 was involved in the development of gastric cancer and may be a potential marker for diagnosis (20). In another study, Cheng *et al* reported that piR-823 reduced tumor activity in gastric cancer cells. These findings suggested that piRNAs mediate cancer progression (21). However, the precise roles and mechanisms of these piRNAs in different types of cancer and processes require further study.

In the present study, we aimed to elucidate the role of piR-651 in NSCLC by examining the expression and potential function of piR-651 in NSCLC.

Materials and methods

Clinical lung cancer samples. Clinical lung cancer samples and adjacent normal tissues from 78 patients with NSCLC were provided by the Xiangya School of Medicine, Central South University (Changsha, China). Informed consent was obtained for all samples, and the study was approved by the institutional review board (Xiangya School of Medicine Research Ethics Committee). All patients included in this study had not received preoperative chemotherapy, radiotherapy or any other therapy. Basic information was collected, including age, gender, clinical manifestation and histological differentiation. The follow-up was from December 1st 2012 and lasted for 24 months. Tissue histology classification was determined according to criteria from the World Health Organization classification of lung tumors (22). The tumor stages were confirmed following the pathological TNM (pTNM) classification (7th edition) of the International Union against Cancer.

Reverse transcription-quantitative polymerase chain reaction (RT-qPCR). Total RNA was extracted using TRIzol reagent (Invitrogen, Carlsbad, CA, USA). RNA (1 μg) was used to synthesize first-strand cDNA. To perform RT-qPCR of piRNA, the miScript SYBR-Green PCR kit provided by Qiagen (Hilden, Germany) was used for reverse transcription, and the PrimeScript™ II 1st Strand cDNA Synthesis kit from Takara (Dalian, China) was used for gene expression detection. The primers used for detecting piRNAs and genes are listed in Table I. The cDNAs were then analyzed using the Applied Biosystems 7500 qPCR System (Life Technologies, Carlsbad, CA, USA). The PCR conditions were as follows: 1 cycle of 94˚C for 2 min; and 40 cycles of 94˚C for 15 sec and 60˚C for 45 sec. The dissociation curves were subsequently performed to verify whether the product was specific. The quantity of the piRNA and gene expression were calculated using the $2^{-\Delta\Delta Ct}$ method.

piRNA northern blot analysis. Total RNA (30 μg) was separated in a 15% denaturing polyacrylamide gel and then transferred onto a GeneScreen Plus Hybridization Transfer membrane (NEN Life Science Products, Inc., Boston, MA, USA) and blotted using a ^{32}P-labeled oligonucleotide. The membrane was then stripped in 0.1X SSPE and hybridized with the probe (piR-651, 5'-GAC GCU UUC CAA GGC ACG GGC CCC UCU CU-3') overnight at 40˚C. The antisense oligonucleotide (5'-AAA ATA TGG AAC GCT TCA CGA-3') of U6 snRNA was used as a loading control. After washing with 2X SSPE containing 1% sodium dodecyl sulfate (SDS), the membrane was exposed to a PhosphorImager screen (Molecular Dynamics, Inc., Sunnyvale, CA, USA) for 20 min.

Fluorescent in situ hybridization. The oligonucleotide probe of piR-651 was synthesized by Sangon Biotech, Co., Ltd. (Shanghai, China) according to the following sequence: piR-651, 5'-GAC GCU UUC CAA GGC ACG-3'. Both the 5' and 3' ends were modified using digoxigenin (DIG) (Life Technologies). A control probe, 5'-AGC GUA UGG AAU UCA GAU CUC A-3' was used as previously described (20).

In situ hybridization for piR-651 was performed on fixed paraffin-embedded sections. Briefly, the samples were fixed in 4% paraformaldehyde at 4˚C overnight following paraffin wax embedding and cut into 8-μm sections. After xylene dewaxing, the samples were digested with 2 ng/ml proteinase K in phosphate-buffered saline (PBS) buffer at 37˚C for 10 min. The samples were then hybridized with 0.5 μM piR-651 probes at 37˚C for 24 h, and then washed with 4X saline sodium citrate (SSC) containing 0.5% Tween-20 for 2 min at room temperature. Finally, an ELF detection kit (Invitrogen) was used to detect green fluorescent signals according to the manufacturer's instructions (Invitrogen). 4',6-diamidino-2-phenylindole (DAPI; 1 μg/ml) (Invitrogen) was used to stain the nuclei. The probe was visualized with DIG combined with anti-DIG-antibody conjugated to alkaline phosphatase and the 5-bromo-4-chloro-3-indolyl-phosphate (BCIP)/nitro-blue tetrazolium (NBT) kit (Invitrogen).

The tissue histology was shown by hematoxylin and eosin (H&E) staining. The paraffin-embedded tissue samples were prepared into 3-5-μm thick slices and were stained with H&E (Beijing Solarbio Science & Technology Co., Ltd., Beijing, China).

Cell culture and transfection. The A549 cell line was obtained from the American Type Culture Collection (ATCC; Manassas, VA, USA). The experimental and control vectors were constructed from the pcDNA3.1(t) plasmid (pc3.1) (Invitrogen) and piRNAs. Briefly, the piR-651 sequence 5'-AGA GAG GGG CCC GUG CCU UGG AAA GCG UC-3' was cloned into the pc3.1 plasmid between the *Bam*HI and *Eco*RI sites to generate pc3.1-piR-651. The sequence 5'-CAG TAT TTT GTG TAG TAC AA-3' was used for the negative control to generate the pc3.1-piR-control.

Table I. Primer sequences used for RT-qPCR.

Gene	Sense (5'→3')	Antisense (5'→3')
piR-651	AGAGAGGGGCCCGTGCCTTG	Provided by miScript SYBR-Green PCR kit
β-catenin	ATGGAACCAGAGAAAAGC	AAGGACTGAGAAAATCCCTG
cyclin D1	CGAGGAGCTGCTGCAAATGG	GGTATCAAAATGCTCCGGAGAGG
cyclin D2	AGCAGCGGGAGAAGCTGTCTCTG	ATGGACGCGTCTCTCTCTTTCGGCC
cyclin D3	TGGATGCTGGAGGTATGTG	CGTGGTCGGTGTAGATGC
CDK2	ATCCGCCTGGACACTGAGACT	TGGAGGACCCGATGAGAATG
CDK4	CACAGTTCGTGAGGTGGCTTTA	TGTCCTTAGGTCCTGGTCTACATG
CDK8	CAAATCCCTTACCCAAAACGAG	TCTGCGGCTGTGATGTGCT
NF-κB	TAAGCAGAAGCATTAACTTCTCT	CCTGCTTCTGTCTCTAGGAGAGTA
Caspase-3	TCTGACTGGAAAGCCGAAACTC	TCCCACTGTCTGTCTCAATGCCAC
ICAM-1	GCAGACAGTGACCATCTACAGCTT	CTTCTGAGACCTCTGGCTTCGT
BCL-2	TGGGATGCCTTTGTGGAACTAT	AGAGACAGCCAGGAGAAATCAAAC
MIF	ACCAGCTCATGGCCTTCG	CTTGCTGTAGGAGCGGTT
MMP-9	ACGCAGACATCGTCATCCAGT	GGACCACAACTCGTCATCGTC
KISS-1	GAGAACTCTTGAGACCGGGAGC	TGGGCTCCCGGTCTCAAGAGTTCTC
RECK	CACAGACCACATGGAGCACAAC	GCTGCCAAGAGCGAAGGACA
EGFR	ACTGCCAGAAACTGACCAAAATC	GCCCTCGGGGTTCACATC
Raf kinase	CTTCTTTGACTATGCGTCGTATGC	GGTGAGGCTGATTCGCTGTG
myc	ACATCATCATCCAGGACTGTATGTG	GGCTGCCGCTGTCTTTGC
HER2	CCCCAAAGCCAACAAAGAAA	GTGTACGAGCCGCACATCCT
p53	ATGGAGGAGCCGCAGTCAGATCCTA	TAGGATCTGACTGCGGCTCCTCCAT
PTEN	TGGAAAGGGACGAACTGGTG	CATAGCGCCTCTGACTGGGA
APC	ATGTACGGGCTTACTAATGACCACT	CACTTCCAACTTCTCGCAACG
CD95	ATGCTGGGCATCTGGACCCT	CAACATCAGATAAATTTATTGCCAC
ST5	GAGTGAGCCCAGCGCCTTCCTCAGG	GAGTGAGCCCAGCGCCTTCCTCAGG
YPEL3	ATGTGTGTGGCCCAGGTCCTGACAG	CTGTCAGGACCTGGGCCACACACAT
ST7	ATTCAATCCTCATGTGCCAAAAT	GATTCAAAGCCCCTTCCACTC
ST14	ACCCTGAGCCCCATGGAGCCCCACG	CGTGGGGCTCCATGGGGCTCAGGGT
GAPDH	TTAGCACCCCTGGCCAAG	GCCATCCACAGTCTTCTGGG

Following vector construction, transfection was performed using Lipofectamine™ 2000 (Invitrogen). The cells were cultured in Dulbecco's modified Eagle's medium with 10% fetal bovine serum (both from Gibco, Gaithersburg, MD, USA) at 37˚C in an incubator with 5% CO_2. Following 24 h of transfection, the cells were subjected to experimental analysis.

Colony formation assay. Colony formation was detected following pc3.1-piR-651 transfection. For each group, the cells were plated into 6-well plates at a density of $1x10^3$ cells/well and incubated for 2 weeks. After washing with PBS three times, the cells were stained using 0.2% crystal violet (GE Healthcare Life Sciences, Little Chalfont, UK) for 20 min at room temperature and observed under an inverted microscope (Nikon Eclipse TS-100F; Nikon, Tokyo, Japan).

Cell viability assay. Cell proliferation was assayed by 3-(4,5-dimethylthiazolyl-2)-2,5-diphenyltetrazolium bromide (MTT) kits (Invitrogen) according to the manufacturer's instructions. Briefly, $2x10^3$ cells/well were plated in 96-well plates. After 24, 48, 72 or 96 h, MTT was added into the wells and plates were incubated at 37˚C for 2 h. Using a VMAX (Molecular Devices, Sunnyvale, CA, USA), the absorbance at 570 and 690 nm (as reference) was detected.

Flow cytometric analysis. To determine the effects of piR-651 on the cell cycle, we performed flow cytometric analysis. Firstly, the cells were fixed with 70% ethanol overnight. After resuspending the cells with 50 μg/ml propidium iodide, the cells were treated with 0.5 μg/ml Annexin V-PE and 0.5 μg/ml 7-amino-actinomycin D (7-AAD) (BD Biosciences, Franklin Lakes, NJ, USA) at room temperature for 15 min and assayed using a FACSCanto flow cytometer (BD Biosciences). The signals of Annexin V, 7-AAD, or both were detected and cell death was analyzed using CellQuestPro software (BD Biosciences).

Western blot analysis. Tissues were homogenized using RIPA lysis buffer (Beyotime, Wuhan, China). The total protein quantity of each sample was analyzed using the bicinchoninic acid (BCA) method (Beyotime). Protein samples (20 μg) were electrophoresed on a 12% SDS polyacrylamide gel and the separated proteins were transferred onto polyvinylidene fluoride membranes (Millipore, Billerica, MA, USA). The membranes were blocked using 4% skim milk for 1 h at room

Table II. Antibodies and dilutions used in the present study.

Protein name	Antibody product code	Dilution	
		Western blot	Immunohistochemistry
Cyclin D1	SAB4502603	1:500	1:100
CDK4	SAB4300695	1:500	1:100
GAPDH	SAB2100894	1:1,000	-

temperature. Primary monoclonal antibodies (antibodies and dilutions are listed in Table II) were purchased from Santa Cruz Biotechnology, Inc., (Santa Cruz, CA, USA) and were incubated with the membranes at 4˚C overnight. GAPDH was used as a loading control. After three washes with TBST buffer (20 mM Tris-HCl, pH 7.6/137 mM NaCl/0.5% Tween-20), the specific protein was detected by a secondary horseradish peroxidase-conjugated goat anti-rabbit antibody (1:2,000; Santa-Cruz Biotechnology, Inc., Heidelberg, Germany). After three washes with TBST buffer, the signals were visualized using an enhanced chemiluminescence detection system (Millipore).

Immunohistochemical analysis. Firstly, 8-μm-thick tissue sections were prepared. The sections were dewaxed and blocked with 4% skim milk. Following incubation with a monoclonal antibody (antibodies and dilutions are listed in Table II) at 4˚C overnight and washing with TBST buffer, the sections were processed with a secondary horseradish peroxidase (HRP)-conjugated goat anti-rabbit antibody (1:200). The specific protein was stained using HRP-conjugated streptavidin (Beyotime) and exposed on photosensitive film (Kodak, Rochester, NY, USA) or with the VersaDoc 3000 imaging system (Bio-Rad Laboratories, Inc., Hercules, CA, USA).

Tumor formation in a nude mouse model. Five-week-old female nude mice were used for the tumor formation experiment. The mice were housed under specific pathogen-free conditions. All animal protocols were approved and monitored by the Ethics Committee of Xiangya School of Medicine, Central South University (Changsha, China). The A549 cells transfected with pc3.1-piR-651 and pc3.1-piR-control were separately inoculated ($2x10^6$ cells) into the dorsal side of the mouse. The tumor volumes were measured and calculated using the equation V=0.5x (width x width x length). The mice were sacrificed 35 days after cell inoculation by dislocation of the cervical vertebrae and the tumor tissues were collected subsequently. The tissues were assayed using RT-qPCR, western blot analysis and immunohistochemistry.

Statistical analysis. All statistical analysis was performed using SPSS v17.0 software. The significant difference among the groups was confirmed by one-way analysis of variance. The correlation of the associations between the expression of piRNAs and various clinicopathologic parameters was calculated according to Spearman. A P-value <0.05 was considered to indicate a statistically significant difference. The Kaplan-Meier survival curves were generated and analyzed with log rank tests with 95% confidence intervals. For the Kaplan-Meier survival analysis over 24 months, 50 patients with relative expression between 1 and 3, as the low expression group, and 50 patients with relative expression between 5 and 6, as the high expression group, were included.

Results

Aberrant expression of piR-651 in NSCLC. The mRNA expression of piR-651 in normal and NSCLC tissues was determined by RT-qPCR, northern blot analysis and *in situ* hybridization. The results showed that piR-651 expression in the cancer lesions of NSCLC patients was significantly higher than that in the adjacent normal tissues (Fig. 1A-C). Furthermore, the upregulation of piR-651 was associated with distal metastasis and disease recurrence (Table III). The Kaplan-Meier survival curves showed that increased piR-651 expression inversely correlated with overall survival (Fig. 1D).

Effects of piR-651 on NSCLC cells. We then analyzed the effects of piR-651 upregulation in NSCLC cells. Firstly, we confirmed that piR-651 expression was increased in the cells transfected with a plasmid expressing piR-651 (Fig. 2A). We then studied cell viability using MTT assays. Cell viability increased significantly following piR-651 overexpression compared with the controls (P<0.05 after 96 h) (Fig. 2B). Additionally, flow cytometry showed that the cells overexpressing piR-651 exhibited significantly reduced levels of apoptosis compared with the controls (Fig. 2C and D). piR-651-overexpressing cells displayed a significantly lower percentage of cells in the G0/G1 phase and significantly higher percentage of cells in the G2/M phase (Fig. 2E), indicating that piR-651 overexpression promotes cell cycle progression. We also found that piR-651-overexpressing cells had a stronger ability to form colonies (Fig. 2F).

Correlation between piR-651 expression and cyclin D1 and CDK4 expression in NSCLC cells. To elucidate the mechanism underlying the effects of piR-651 in NSCLC cells, the expression patterns of lung cancer-related genes were examined after overexpression of piR-651. The cancer-promoting genes induced by piR-651 overexpression included β-catenin, cyclin D, CDK, NF-κB, ICAM and MIF. Similarly, several oncogenes, including cyclin D, CDK, MMP-9, KISS-1, RECK, EGFR, Raf kinase, myc and HER2, showed significantly higher expression after piR-651 overexpression. By contrast, the expression levels of cancer suppressor genes, such as p53, PTEN, APC, CD95, ST5, YPEL3, ST7 and ST14, were decreased with higher expression of piR-651 (Fig. 3A).

Of all the examined genes, only cyclin D1 and CDK4 showed a high correlation with piR-651 (R^2>0.5 and P<0.05). Cyclin D1 expression positively correlated with piR-651 expression (R^2=0.834 and P<0.05) (Fig. 3B). Similarly, CDK4 expression positively correlated with piR-651 expression (R^2=0.721 and P<0.05) (Fig. 3B). Western blot analysis also revealed that the protein expression of cyclin D1 and CDK4 increased following the upregulation of piR-651 (Fig. 3C).

Correlation between piR-651 expression and cyclin D1 and CDK4 expression in NSCLC tissues. A positive correlation (R^2=0.771 and P<0.05) between piR-651 expression and

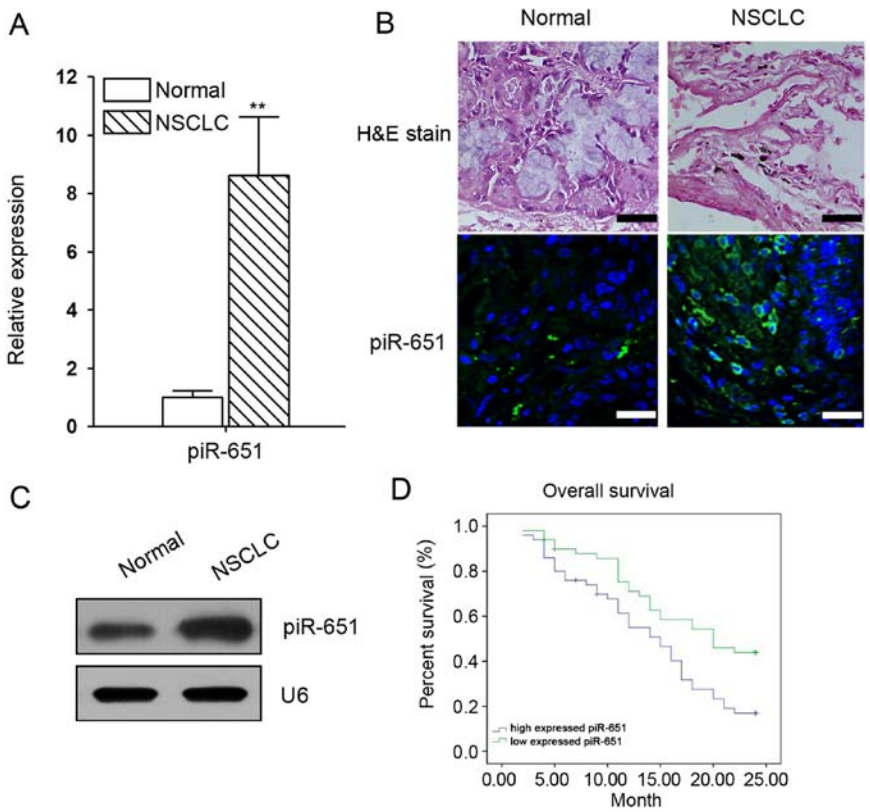

Figure 1. Abnormal expression of piR-651 in non-small cell lung carcinoma (NSCLC) tissues. (A) Relative expression of piR-651 was higher in the NSCLC tissues compared with that in the normal tissues (data are expressed as the means ± SD, n=78, **P<0.01) according to RT-qPCR analysis. (B) *In situ* hybridization results indicated that piR-651 was highly expressed in the NSCLC tissues. Scale bar, 50 μm. (C) Higher expression of piR-651 in NSCLC tissue compared with normal tissue was determined by northern blot analysis. (D) Overall survival with low (relative expression between 1 and 3) and high (relative expression between 5 and 6) expression of piR-651.

Table III. Analysis of the correlation between piR-651 expression in NSCLC tissues and the patient clinicopathological characteristics.

Variable	N	Median piR-651 expression (range)	P-value (piR-651)
Age (years)			
≤50	36	5.60 (0.89-12.42)	0.89
>50	42	4.41 (0.74-10.78)	
Gender			
Male	56	6.02 (0.89-10.78)	0.45
Female	22	4.26 (0.74-12.42)	
T stage			
T1/T2	52	3.18 (0.74-7.65)	0.03
T3/4	26	7.62 (3.62-12.42)	
Histologic grade			
I-II	55	2.23 (0.74-4.69)	0.02
III-IV	23	8.07 (4.54-12.42)	
Metastasis			
No (M0)	50	2.53 (0.74-4.49)	0.01
Yes (M1)	28	9.62 (4.48-12.42)	
Tumor size			
≤5 cm	63	3.88 (0.74-5.47)	0.01
>5 cm	15	8.69 (4.49-12.42)	

NSCLC, non-small cell lung carcinoma.

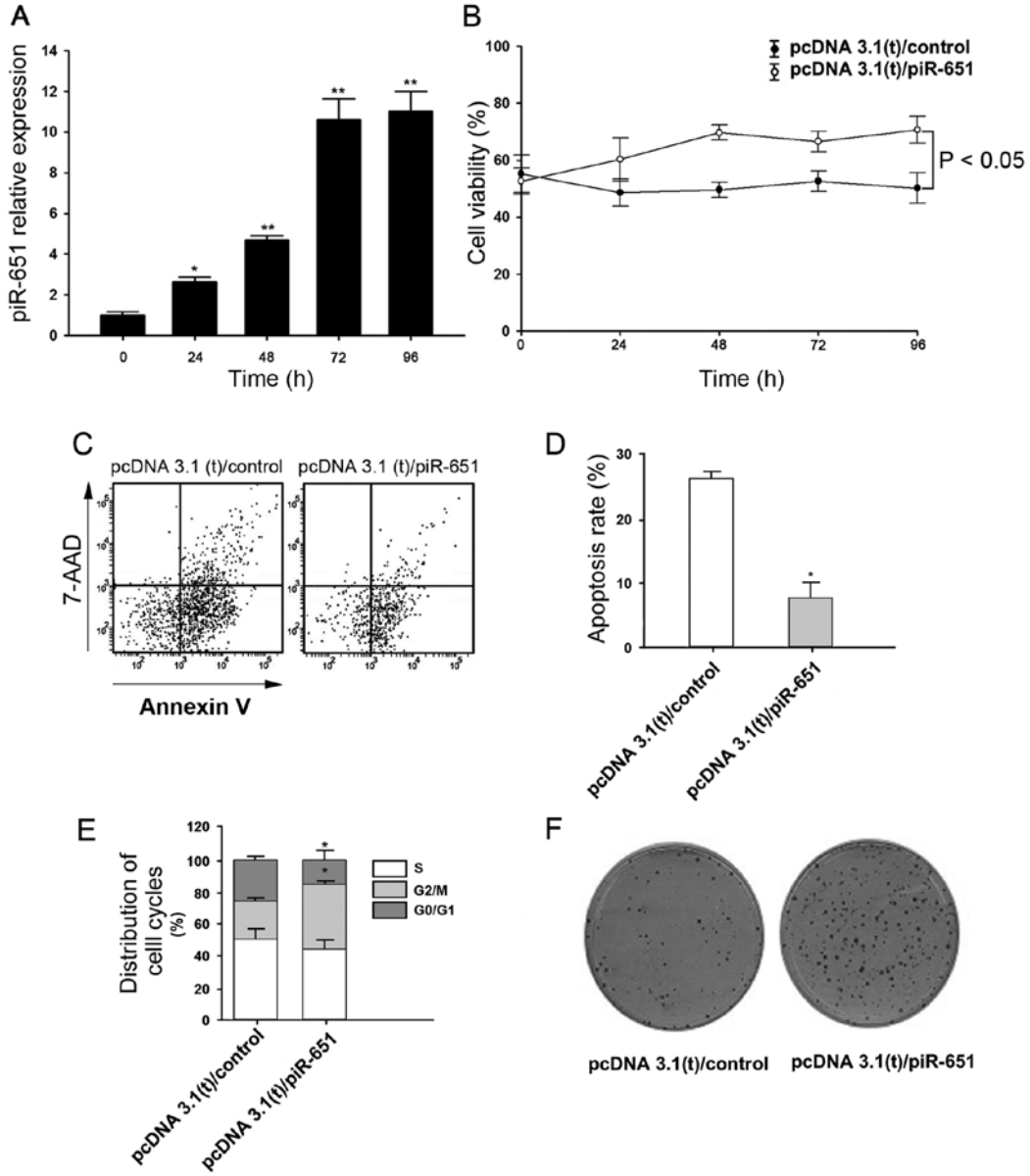

Figure 2. Cell biological activities following piR-651 overexpression in non-small cell lung carcinoma (NSCLC) cells. (A) The increased expression of piR-651 following transfection (n=3, *P<0.05 and **P<0.01 compared with the control). (B) Cell viability was determined by MTT assay. Cell viability was increased in piR-651-overexpressing cells (data are expressed as the means ± SD, n=3). (C) Flow cytometric analysis of the NSCLC cells after piR-651 overexpression. (D) Apoptosis rates were calculated from flow cytometry data (*P<0.05, compared with the control, data are expressed as the means ± SD, n=3). (E) The percentage of NSCLC cells in each phase of the cell cycle (*P<0.05, compared with the control, data are expressed as the means ± SD, n=3). (F) Colony formation assay of NSCLC cells in the control and the piR-651-overexpressing groups.

cyclin D1 was observed in the NSCLC tissues from patients. Moreover a similar positive correlation between piR-651 expression and CDK4 (R^2=0.727 and P<0.05) was also shown in these tissues (Fig. 4A). To determine whether piR-651, cyclin D1 and CDK4 are involved in metastasis, the expression levels from patients at the M0 and M1 stage (n=3) were assayed (Fig. 4B). The expression levels of piR-651, cyclin D1 and CDK4 were higher in the M1 stage patients compared with the M0 stage patients (Fig. 4C), indicating that increased levels of piR-651 induced cyclin D1 and CDK4 and thus, promoted metastasis.

piR-651 promotes tumor growth in vivo. In order to further examine the relevance of our *in vitro* findings with regard to NSCLC tumorigenesis *in vivo*, we injected A549 cells transfected with control sequences or piR-651 plasmids into nude mice to generate xenograft models and monitored tumor growth. In tumors injected with piR-651-overexpressing cells, the tumor volume and tumor weight were higher compared with the controls (P<0.05 after 5 weeks) (Fig. 5A and B), which was consistent with our *in vitro* findings. The tissue sections also showed that piR-651 triggered NSCLC tumorigenesis *in vivo* (Fig. 5C). At 5 weeks after cell implantation, higher expression of piR-651 was observed in tumor tissues evaluated by RT-qPCR and northern blot analysis (Fig. 5D).

Consistent with our results described above, the overexpression of piR-651 led to an increased level of cyclin D1 and CDK4 in the xenograft tumor tissues (Fig. 6). Thus, these

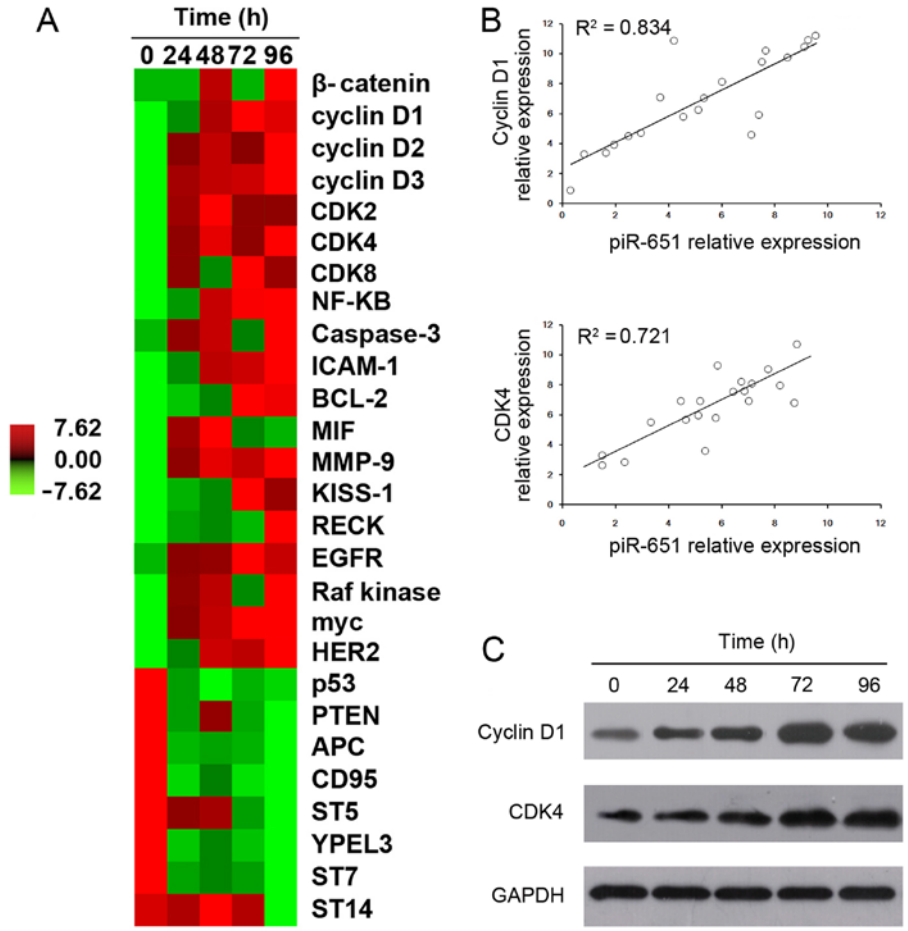

Figure 3. Correlation between piR-651 expression and cyclin D1 and CDK4 expression in non-small cell lung carcinoma (NSCLC) cells. (A) The heat map compares the expression of differentially expressed cancer-promoting genes and oncogenes across different time-points after transfection with piR-651. (B) Positive correlations between cyclin D1 and CDK4 expression and piR-651 expression in 20 wells of the transfected cells. (C) Protein levels of cyclin D1 and CDK4 following piR-651 overexpression in NSCLC cells.

results from the nude mouse xenograft model demonstrate that piR-651 promotes NSCLC tumorigenesis *in vivo* through the cyclin D1 and CDK4 pathway.

Discussion

A novel class of small RNAs, referred to as piRNAs, have been identified in mouse germline cells (23,24). Notably, it has been demonstrated that the overexpression of PIWI and piRNAs results in the abnormal development of gonads in vertebrates (25,26). In humans, the increased expression of Hiwi, a homolog of Piwil1, was found to correlate with the risk of cancer-related death in the pancreas of male individuals (27). A previous study has suggested that piRNAs were highly expressed in gastric cancer tissues (17). These findings have demonstrated that piRNAs are potential diagnostic indicators of gastric cancer. In the present study, our findings confirmed that piR-651 participates in the development of NSCLC.

The present study demonstrated high piR-651 expression in patients with NSCLC. The overall survival curves suggested that the high expression of piR-651 was associated with a higher risk of death. These results are similar to the findings from a study of gastric cancer showing that piR-651 was upregulated in gastric cancer. In addition, by inhibiting piR-651, gastric cancer cells were suppressed, which to the best of our knowledge, was the first demonstration of a novel class of small RNAs capable of regulating the progression of cancer (20). Based on the observations of similar expression levels of piR-651 in patients with gastric cancer and NSCLC, the regulatory mechanisms controlled by these piRNAs need to be elucidated.

Our results showed that following the overexpression of piR-651 in NSCLC cells, cell viability was significantly increased. A previous study has demonstrated that upregulating piR-651 may promote cancer metastasis in gastric cell lines and downregulating piR-651 arrested the cells in the G2/M phase (20). However, current information regarding the effects of piR-651 on the activities of cancer cells is limited. Whether the effects of piR-651 on cancer cells are specific to different types of cancer remains unknown. Our findings suggest that piR-651 exhibits similar effects in NSCLC as in gastric cancer cells in terms of promoting cell viability. In addition, upregulating piR-651 in NSCLC cells significantly reduced the number of cells in the G0/G1 phase and increased the number of cells in the G2/M phase, indicating a regulatory function for piR-651 in cell proliferation.

Our results showed that the expression of oncogenes was induced and that of the cancer suppressor genes was reduced

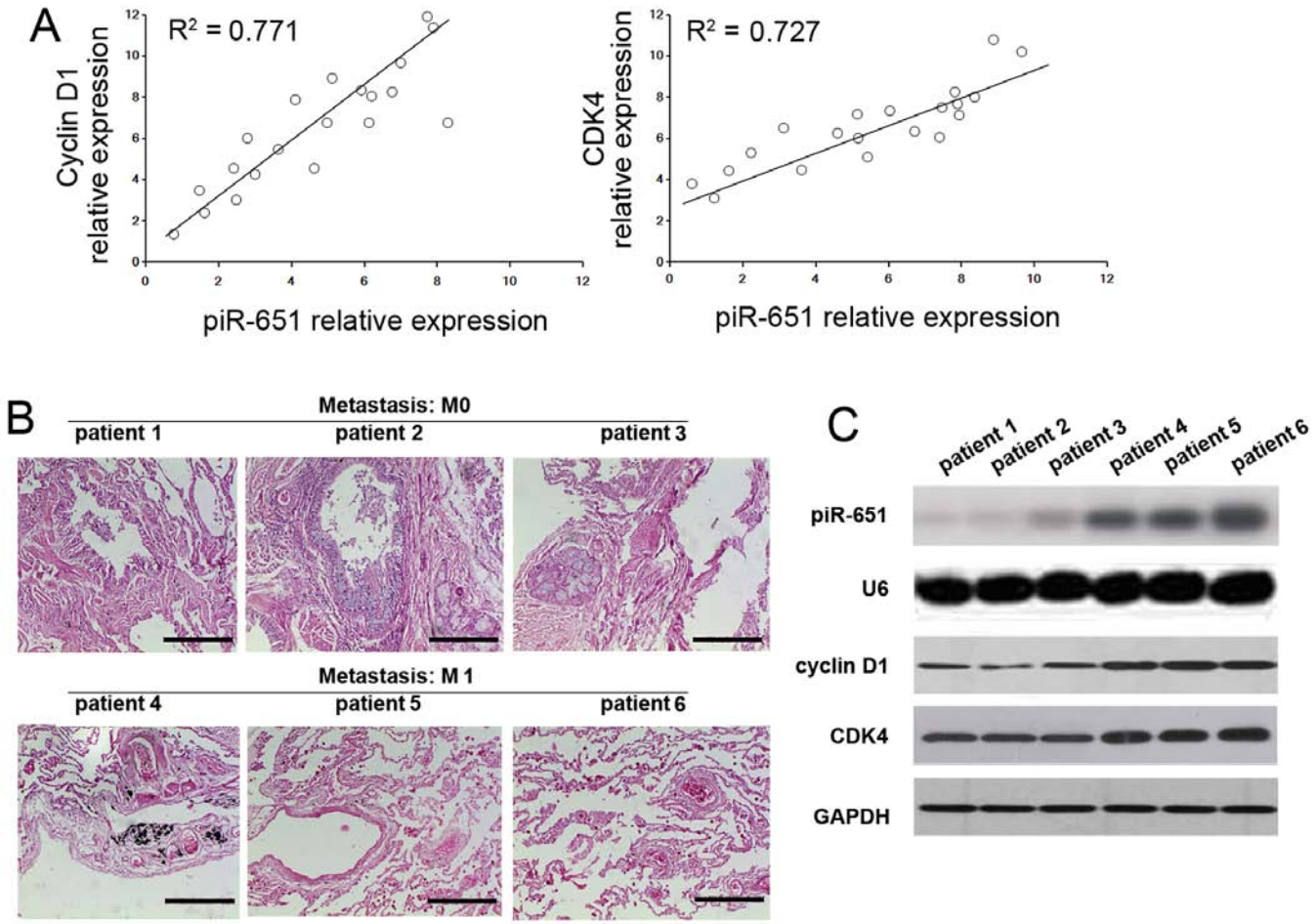

Figure 4. Correlation between piR-651 expression and cyclin D1 and CDK4 expression in non-small cell lung carcinoma (NSCLC) patients. (A) Positive correlations of cyclin D1 and CDK4 with piR-651 in 20 patients with NSCLC. (B) Histology of NSCLC samples from six patients (three were in M0 metastasis stage; three were in M1 metastasis stage confirmed by the TNM staging system). Scale bar, 200 μm. (C) Expression levels of piR-651 (detected by northern blot analysis), cyclin D1 (detected by western blot analysis), and CDK4 (detected by western blot analysis) were increased in M1 tissues compared with M0 tissues.

by piR-651. To the best of our knowledge, this is the first demonstration that a single piRNA is capable of regulating the expression of a wide panel of cancer-related genes. Furthermore, the correlation between piR-651 expression and the genes was analyzed. Notably, *in vivo* and *in vitro* studies showed that only cyclin D1 and CDK4 positively correlated with piR-651 expression. Cyclin D1 and CDK4 drive cell cycle progression through the G1 checkpoint. The upregulation of cyclin D1 and CDK4 promoted cell cycle progression, which led to cell proliferation. Thus, our findings revealed that piR-651 promotes the cell cycle by regulating cyclin D1 and CDK4.

The mechanism of gene regulation by miRNAs has been intensively investigated. However, as a novel class of non-coding, small RNAs, the regulation of genes by piRNAs remains unclear. Robine *et al* have reported the existence of a 3' untranslated region (3'UTR) conserved pathway of piRNAs, suggesting a similar transcriptional regulating function for piRNAs as for miRNAs by acting on the 3'UTR (28). Nevertheless, there is no evidence for any direct binding between piRNAs and transcripts. The molecular mechanisms underlying the regulatory effects of piR-651 on cyclin D1 and CDK4 remain unknown and warrant further investigation.

Finally, our results demonstrated that the injection of piR-651-transfected cells significantly promoted increases in tumor volume and tumor weight. The overexpression of piR-651 lasted for 5 weeks. Thus, we propose that piR-651 may function as an oncogene in NSCLC. Previous studies have demonstrated a role for piR-651 in promoting tumorigenesis. However, whether single piRNAs play a direct role in different types of cancer is currently unknown. Notably, upregulation of cyclin D1 and CKD4 was found in the group injected with piR-651-transfected cells, which confirmed the function of piR-651 as a modulator of the cell cycle. Taken together, this evidence indicates that piRNAs may play a crucial role in human disease.

In conclusion, the present study has demonstrated that piR-651 is associated with the progression of NSCLC. The high expression of piR-651 was associated with a higher risk of death in patients with NSCLC. The viability and cell cycle progression of NSCLC cells were also regulated by piR-651. The expression levels of cyclin D1 correlated with piR-651 expression. In addition, tumor formation was promoted by injecting nude mice with piR-651-overexpressing A549 cells. Our findings suggest that piR-651 may have applications as

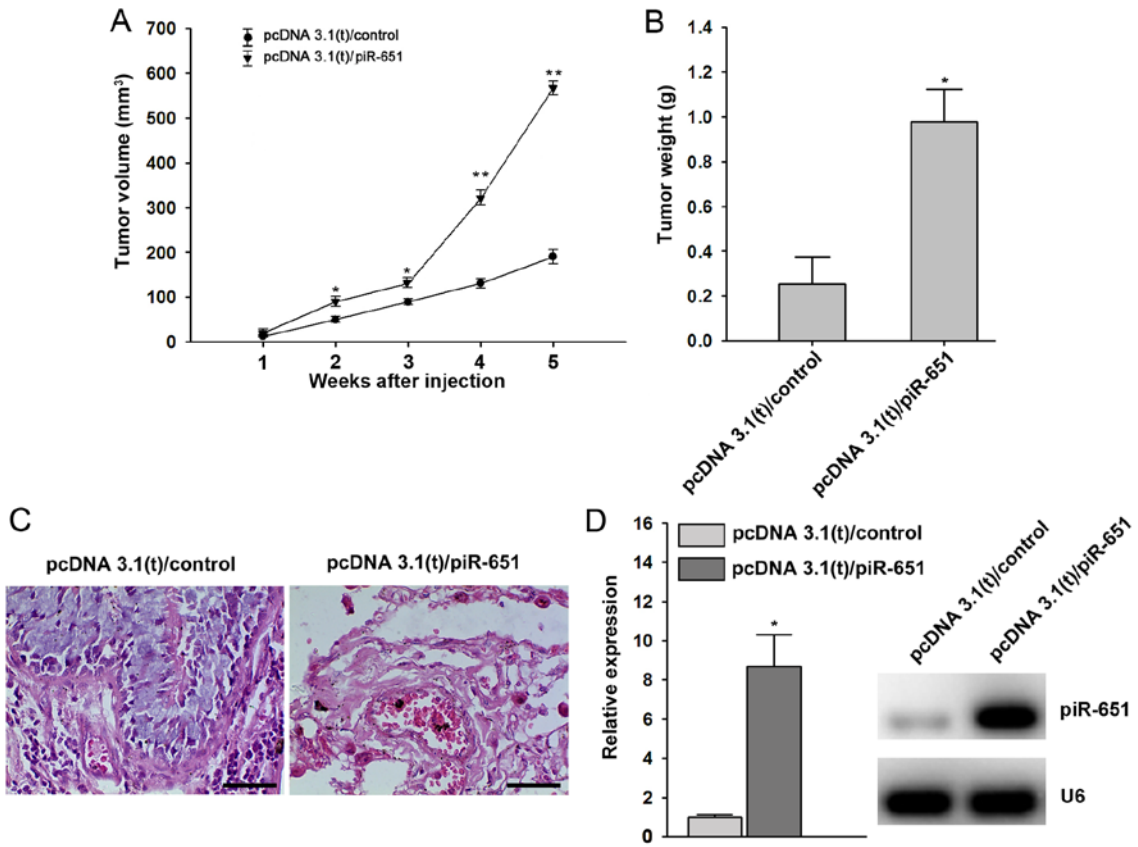

Figure 5. piR-651 overexpression promotes tumor formation. (A) Volume of xenograft tumors derived from A549 cells overexpressing piR-651 or control sequence in nude mice (data are expressed as the means ± SD, n=6, *P<0.05 and **P<0.01). (B) The weight of xenograft tumors in nude mice (data are expressed as the means ± SD, n=6, *P<0.05). (C) Histology of xenograft tumors derived from A549 cells overexpressing piR-651 and control sequences. (D) Expression levels of piR-651 in xenograft tumor tissues (data are expressed as the means ± SD, n=6, *P<0.05).

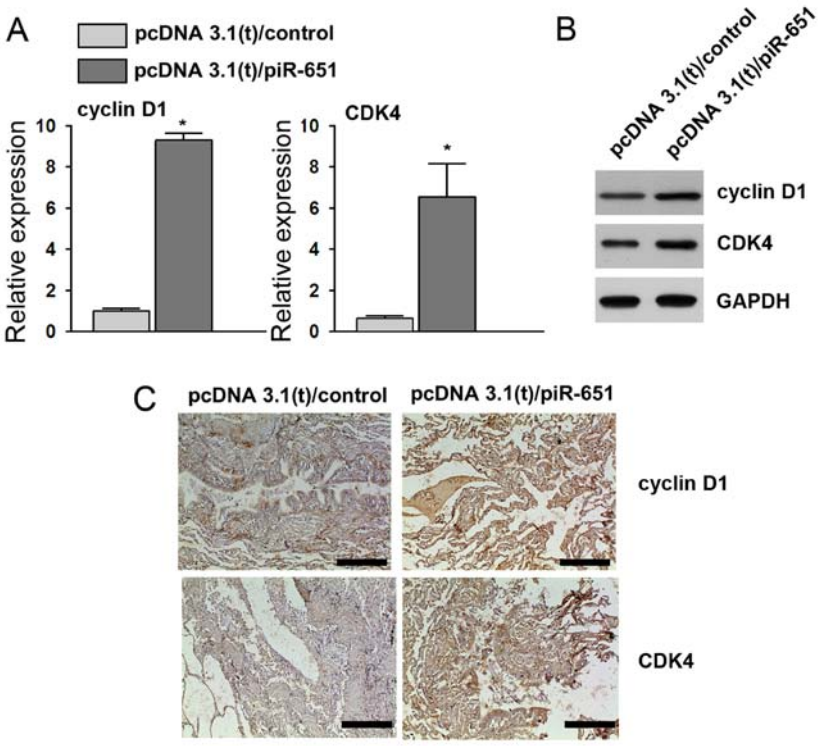

Figure 6. piR-651 overexpression promotes expression of cyclin D1 and CDK4 in xenograft tumor tissues. (A) Relative expression of cyclin D1 and CDK4 was higher after piR-651 overexpression compared with the control (data are expressed as the means ± SD, n=6, *P<0.05). (B) Western blot analysis showed higher expression of cyclin D1 and CDK4 in xenograft tumor tissues derived from A549 cells overexpressing piR-651 compared with the control. (C) Immunohistochemical assay of cyclin D1 and CDK4 in xenograft tumor tissues. Scale bar, 100 μm.

a potential diagnostic indicator and therapeutic target in the management of NSCLC.

Acknowledgements

This study was supported by the Hunan Provincial Natural Science Fund of China (grant no. 13JJ6092).

References

1. Goldstraw P, Ball D, Jett JR, Le Chevalier T, Lim E, Nicholson AG and Shepherd FA: Non-small-cell lung cancer. Lancet 378: 1727-1740, 2011.
2. Suntharalingam M, Paulus R, Edelman MJ, Krasna M, Burrows W, Gore E, Wilson LD and Choy H: Radiation therapy oncology group protocol 02-29: a phase II trial of neoadjuvant therapy with concurrent chemotherapy and full-dose radiation therapy followed by surgical resection and consolidative therapy for locally advanced non-small cell carcinoma of the lung. Int J Radiat Oncol Biol Phys 84: 456-463, 2012.
3. Sharma S, Kelly TK and Jones PA: Epigenetics in cancer. Carcinogenesis 31: 27-36, 2010.
4. Sandoval J and Esteller M: Cancer epigenomics: beyond genomics. Curr Opin Genet Dev 22: 50-55, 2012.
5. Schlesinger F, Smith AD, Gingeras TR, Hannon GJ and Hodges E: De novo DNA demethylation and noncoding transcription define active intergenic regulatory elements. Genome Res 23: 1601-1614, 2013.
6. Lopez-Serra P and Esteller M: DNA methylation-associated silencing of tumor-suppressor microRNAs in cancer. Oncogene 31: 1609-1622, 2012.
7. Levin HL and Moran JV: Dynamic interactions between transposable elements and their hosts. Nat Rev Genet 12: 615-627, 2011.
8. Chénais B: Transposable elements and human cancer: a causal relationship? Biochim Biophys Acta 1835: 28-35, 2013.
9. Senti KA and Brennecke J: The piRNA pathway: a fly's perspective on the guardian of the genome. Trends Genet 26: 499-509, 2010.
10. Ambros V and Chen X: The regulation of genes and genomes by small RNAs. Development 134: 1635-1641, 2007.
11. Houwing S, Kamminga LM, Berezikov E, Cronembold D, Girard A, van den Elst H, Filippov DV, Blaser H, Raz E, Moens CB, *et al*: A role for Piwi and piRNAs in germ cell maintenance and transposon silencing in Zebrafish. Cell 129: 69-82, 2007.
12. Aravin AA, Sachidanandam R, Girard A, Fejes-Toth K and Hannon GJ: Developmentally regulated piRNA clusters implicate MILI in transposon control. Science 316: 744-747, 2007.
13. Seto AG, Kingston RE and Lau NC: The coming of age for Piwi proteins. Mol Cell 26: 603-609, 2007.
14. Yan Z, Hu HY, Jiang X, Maierhofer V, Neb E, He L, Hu Y, Hu H, Li N, Chen W and Khaitovich P: Widespread expression of piRNA-like molecules in somatic tissues. Nucleic Acids Res 39: 6596-6607, 2011.
15. Siddiqi S and Matushansky I: Piwis and piwi-interacting RNAs in the epigenetics of cancer. J Cell Biochem 113: 373-380, 2012.
16. Li L, Yu C, Gao H and Li Y: Argonaute proteins: potential biomarkers for human colon cancer. BMC Cancer 10: 38, 2010.
17. Cui L, Lou Y, Zhang X, Zhou H, Deng H, Song H, Yu X, Xiao B, Wang W and Guo J: Detection of circulating tumor cells in peripheral blood from patients with gastric cancer using piRNAs as markers. Clin Biochem 44: 1050-1057, 2011.
18. Al-Janabi O, Wach S, Nolte E, Weigelt K, Rau TT, Stöhr C, Legal W, Schick S, Greither T, Hartmann A, *et al*: Piwi-like 1 and 4 gene transcript levels are associated with clinicopathological parameters in renal cell carcinomas. Biochim Biophys Acta 1842: 686-690, 2014.
19. Ye Y, Yin DT, Chen L, Zhou Q, Shen R, He G, Yan Q, Tong Z, Issekutz AC, Shapiro CL, *et al*: Identification of Piwil2-like (PL2L) proteins that promote tumorigenesis. PLoS One 5: e13406, 2010.
20. Cheng J, Guo JM, Xiao B-X, Miao Y, Jiang Z, Zhou H and Li QN: piRNA, the new non-coding RNA, is aberrantly expressed in human cancer cells. Clin Chim Acta 412: 1621-1625, 2011.
21. Cheng J, Deng H, Xiao B, Zhou H, Zhou F, Shen Z and Guo J: piR-823, a novel non-coding small RNA, demonstrates in vitro and in vivo tumor suppressive activity in human gastric cancer cells. Cancer Lett 315: 12-17, 2012.
22. Brambilla E, Travis WD, Colby TV, Corrinz B and Shimosato Y: The new World Health Organization classification of lung tumours. Eur Respir J 18: 1059-1068. 2001.
23. Girard A, Sachidanandam R, Hannon GJ and Carmell MA: A germline-specific class of small RNAs binds mammalian Piwi proteins. Nature 442: 199-202, 2006.
24. Aravin A, Gaidatzis D, Pfeffer S, Lagos-Quintana M, Landgraf P, Iovino N, Morris P, Brownstein MJ, Kuramochi-Miyagawa S, Nakano T, *et al*: A novel class of small RNAs bind to MILI protein in mouse testes. Nature 442: 203-207, 2006.
25. Houwing S, Berezikov E and Ketting RF: Zili is required for germ cell differentiation and meiosis in zebrafish. EMBO J 27: 2702-2711, 2008.
26. Pan Y, Hu M, Liang H, Wang JJ and Tang LJ: The expression of the PIWI family members miwi and mili in mice testis is negatively affected by estrogen. Cell Tissue Res 350: 177-181, 2012.
27. Grochola LF, Greither T, Taubert H, Möller P, Knippschild U, Udelnow A, Henne-Bruns D and Würl P: The stem cell-associated Hiwi gene in human adenocarcinoma of the pancreas: expression and risk of tumour-related death. Br J Cancer 99: 1083-1088, 2008.
28. Robine N, Lau NC, Balla S, Jin Z, Okamura K, Kuramochi-Miyagawa S, Blower MD and Lai EC: A broadly conserved pathway generates 3'UTR-directed primary piRNAs. Curr Biol 19: 2066-2076, 2009.